RSC Advances

ROYAL SOCIETY
OF **CHEMISTRY**

www.rsc.org/advances

Journal Name

ARTICLE

Three-dimensional orientation of Poly(L-lactide) crystals under uniaxial drawing

E. Lizundia[a], A. Larrañaga[b], J. L. Vilas[a,c] and L. M. León[a,c]

In this work the effects of three-dimensional crystal development upon polymer stretching are investigated. Poly (L-lactide) has been selected as a model semicrystalline polymer owing to its high chain stereoregularity which enables its crystallization by strain-induced mechanism. Specimens containing a bulk crystal volume fraction up to 55.5% have been obtained. Fourier transform infrared spectroscopy (FTIR) proves the development of more densely packed domains with strong dipole–dipole interactions for the more stretched PLLA. X-ray diffraction (XRD) has been implemented to obtain insights about the occurring micro-structural changes. Additionally, to determine macromolecular orientations texture analysis using XRD has been performed via pole figure measurements, which demonstrate that crystalline domains are transformed from fibrils into planar spherulites as stretching evolves. It is proposed that the strain-induced crystallization mechanism upon stretching is governed by the decrease of the number of degrees of freedom for crystallization process when the compression is enough to limit one of the possible orientations. Obtained morphological evidences for the suggested crystal transformations by field emission scanning electron microscopy (FE-SEM) further confirm our hypothesis. In the future, the analysis of three-dimensional strain-induced crystal orientation would result of prime interest for other commonly used semicrystalline polymers such as isotactic polypropylene (iPP), polyethylene (PE), polyethylene terephthalate (PET) and polyamide 66 (nylon).

Introduction

Nowadays thermoplastic materials represent one of the most commonly used materials for automotive, packaging, healthcare, optics, telecommunication industries and so on. Among all the thermoplastic materials that could be easily processed by the conventional technologies, polylactides show a bright future. Provided their cost competitive character, their mechanical performance better than polystyrene (PS) and its physico-chemical similarities with polyethylene terephthalate (PET),[1,2] they are considered of special interest from an ecological point of view due to its biobased character. Indeed, they belong to biodegradable and biocompatible polyesters that are interesting candidates to replace traditional polymers derived from petrochemical resources.[3] As occurs in other polymers, the presence of an asymmetric carbon in its structure results in the formation of two stereoisomers, yielding three morphologically different polymers.[4] Among all of them, the semicrystalline Poly (L-lactide) (PLLA) shows the brightest future due to its tunable phase-structure and physico-chemical properties.[5] Unfortunately, some of the functional properties of PLLA remain insufficient, limiting its implementation in many application areas. For instance, PLA shows poor water barrier and

medium gas barrier properties,[6,7] slow crystallization rate,[8] quick structural relaxation when it is used at ambient temperature,[9] poor thermal stability,[10] and low mechanical performance.[5]

As a result of the high chain stereoregularity of PLLA,[11] it could be easily crystallized by strain-induced and thermally-induced mechanisms.[4,5,12,13] In this sense, PLLA stretching could be seen as a cost-effective and quick route to overcome aforementioned drawbacks since the development of oriented crystalline domains would yield improved barrier, mechanical, thermal and optical properties. Indeed, polymer stretching plays a crucial role in common polymer processing technologies. During these fabrication processes such as extrusion blowing, polymer chains are aligned to form crystalline regions which depend upon the applied stretching ratio. It has been proven that the barrier properties of semicrystalline thermoplastics could be increased upon drawing, yielding improved materials for packaging applications. Thus, understanding how Poly(L-lactide) crystals are oriented upon drawing results of prime interest from both academic and industrial point of view. Although PLLA is already a well known semicrystalline polymer, its full mechanical potential has not been achieved because crystalline domains are usually isotropically distributed over the whole bulk material. In fact, it has been demonstrated that the strain-induced crystallization achieved during the stretching notably improves the mechanical and H_2O and O_2 barrier properties of resulting materials in regard with their non-stretched counterparts.[14]

Differential scanning calorimetry (DSC) is a common thermo-analytical technique which enables the quantitative determination of crystalline phase within the bulk polymer.[15] X-ray diffraction has been improved nowadays opening new measurement options, for example giving clear and fast crystal orientation distributions for the crystals.[14,16] Additionally, non-destructive Fourier transform

a. Macromolecular Chemistry Research Group (LABQUIMAC). Dept. of Physical Chemistry. Faculty of Science and Technology. University of the Basque Country (UPV/EHU), Spain.
b. SGIker, General Research Services, University of the Basque Country (UPV/EHU), Spain.
c. Basque Center for Materials, Applications and Nanostructures (BCMaterials), Parque Tecnológico de Bizkaia, Ed. 500, Derio 48160, Spain.
E-mail: Erlantz.liizundia@ehu.eus

infrared spectroscopy (FTIR) is of key relevance to study conformational changes occurring in polymeric materials because it enables the determination of crystalline phases with distinct intermolecular interactions.[17] More precisely, in the case of polylactides the carbonyl (C=O) stretching band remains almost uncoupled from the vibrational modes of the backbone chain,[4] providing further information on the conformational changes occurring upon stretching PLLA films.

To the best of our knowledge no previous works have been devoted to the systematic understanding how the structure and conformation of crystalline phases change during the stretching of biopolymers such as PLLA. Indeed, up to now, the use of Pole figures to determine the distribution of crystallographic orientations in the field of materials science has been mainly focused to semiconductor, inorganic materials or depositions such as CuO,[18] [Ca$_2$CoO$_3$]$_{0.62}$[CoO$_2$] (CCO),[19] TiO$_2$,[20] SnS...[21] Thorough this work we have found interesting results towards the complete understanding of the occurring chain orientation effects during PLLA stretching, for which very scarce studies could be found in polymer science. Additionally, one of the advantages that presents PLLA is that it could be utilized as a model polymer to extent obtained findings to other commonly used semicrystalline polymers such as isotactic polypropylene (iPP), polyethylene (PE), polyethylene terephthalate (PET), polyamide 66 (nylon)...

In this work we attempt to evaluate the conformational development of bio-based PLLA in differently stretched configurations. DSC has been implemented to evaluate the obtained bulk phase-structure changes. Additionally, micro-structural changes occurring upon stretching have been monitored by WAXD. Pole figure analysis has been carried out to give further insights on the occurring crystallization of PLLA during uniaxial stretching process. Finally, by means of FTIR the occurring conformational changes upon drawing have been analyzed. In overall, this work aims to set up a relationship between the common stretching of PLLA during its conformation and the resulting microstructure with the aid to three-dimensional tools. In accordance with the 12 Principles of Green Chemistry,[22] oriented PLLA could yield a new generation of ecologically friendly materials with improved functional properties, which would help to address the depletion of fossil resources that our society is facing nowadays.

Experimental

Materials and sample preparation

PLLA with a weight-average molecular weight (M_w) of 110.000g/mol and a polydispersity index (M_w/M_n) of 1.81 has been kindly provided by Purac Biochem (The Netherlands). After vacuum drying of PLLA pellets at 60ºC for 24h, 400µm thick films were fabricated by hot pressing at 180ºC for 5 min at a pressure of 150 MPa. Films were solidified by sinking molten nanocomposites in an iced water bath to avoid any crystalline development during sample preparation. Specimens were punched out from films according to ISO 527-1:2012, specimen type 5A (http://www2.ulprospector.com/property_descriptions/ISO527-1-2.asp).

Hot stretching

In order ensure the elastomeric behavior of PLLA and to prevent any crystallization induced by temperature during the drawing process, 3mm width and 30mm long specimens were uniaxially drawn just above T_g for different elongations using a AGS-X

Universal Testing Machine from Shimadzu at a constant jack speed of 5 mm s^{-1} (16.6% s^{-1}). Samples were heated at 65ºC with the aid of an infrared incandescent reflector lamp (Philips IR250 RH IR2). Sandpaper was place between clamp and specimen in order to avoid creating stress concentrations at the junctions with clamps. Once films were completely stretched, samples were cooled to room temperature in the stretched conformation and they were removed so as to ensure that samples do not suffer any shrinkage effect. Four dumbbell-shaped specimens have been stretched to ensure the reproducibility of the performed experiments. A maximum stretching ratio of 340% has been applied. For comparison purposes, PLLA has been submitted to several cold-crystallization treatments (ranging from 60ºC to 150ºC). Gel permeation chromatograph (GPC) results reveal an almost negligible decrease of molecular weight upon melt processing, while hot stretching does not modify the molecular weight of PLLA.

Differential scanning calorimetry (DSC)

The thermal behavior of the samples was determined using a Mettler Toledo DSC 822e calorimeter under nitrogen atmosphere (30 ml/min). Samples 8±1 mg were sealed in an aluminum pan, heated from -20ºC to 200ºC at a rate of 10ºC/min in order to determine thermal transitions changes induced by drawing process. The crystalline fraction X_c (%) attributable to the PLLA crystallization during the corresponding heat treatment was determined as follows:[15]

$$X_c(\%) = \frac{\Delta H_f - \Delta H_c}{\Delta H_f^0} \cdot 100 \qquad (1)$$

where ΔH_f and ΔH_c are respectively the enthalpy of fusion and cold crystallization of the samples determined on the DSC. ΔH_f^0 = 93 J/g was taken as the heat of fusion of an infinitely thick PLLA crystal.[23] Accordingly, the volume fractional amount of crystallinity (ϕ_c) could be computed as follows according to:

$$\phi_c(\%) = \frac{X_c}{X_c + (1 - X_c)\dfrac{\rho_c}{\rho_a}} \cdot 100 \qquad (2)$$

where ρ_c and ρ_a are the densities of fully crystalline PLLA comprising only α-form (1.285g/cm^3) and fully amorphous PLLA (1.245g/cm^3).[24] When comparing 2D Pole figures with bulk crystallinity of specimens, volume fractions are taken into account because X-ray diffraction accounts for volume fraction crystallinity.

Fourier transform infrared spectroscopy (FTIR)

Infrared spectra in attenuated total reflectance (ATR) mode were recorded on a Shimadzu FTIR-8400s spectrophotometer using a MIRacle ZnSe ATR accessory. Each IR spectrum consisted of 32 scans in the range 600–4000cm^{-1} with a 2 cm^{-1} resolution. Average values over three replicates are reported for each drawing ratio.

X-Ray Diffraction (XRD)

Standard X-ray Diffraction data were collected by using a Philips X´Pert Pro automatic diffractometer operating at 40 kV and 40 mA, in theta-theta configuration, secondary monochromator with Cu-Kα radiation (λ = 1.5418 Å) and a PIXcel solid state detector (active length in 2ϑ 3.347º). Data were collected from 5 to 50° 2ϑ (step size = 0.026 and time per step = 85s) at RT. A fixed divergence and antiscattering slit giving a constant volume of sample illumination were used. Texture evaluation of the samples was measured using a Bruker D8 Discover diffractometer equipped with a Cr Twist tube, V filter (λ = 2.2910 Å), PolyCap^{TM} system for parallel been generation

ARTICLE

(divergence of 0.25°), and a 1-D LynxEye detector (active length in 2θ 3º). The samples were mounted on an Eulerian Cradle with automatic controlled X-Y-Z stage. Data were collected for (110)/(200), (210) and (310)/(020) reflections at 24.50, 31.95 and 43.15 º in 2Theta, respectively (using a fixed mode and time per orientation of 20 s). The data collection in standard mode with 5º of δ was measured for full circle 0-360 incr. 5º in Phi (φ) and 0-75 incr. 5º in Psi(ψ) range, giving 2079 total orientations.

Morphological characterization

The crystalline morphology of specimens has been analyzed in a Hitachi S-4800 field emission scanning electron microscope (FE-SEM) at an acceleration voltage of 5 kV. Cryogenically fractured surfaces were gold-coated in an Emitech K550X sputter coater.

Results and discussion

Crystalline development under stretching

Since PLLA is a rather brittle material, it's stretching needs to be carried out in the elastomeric region but under a temperature low enough to inhibit the development of any temperature-induced crystallinity. To that end, PLLA has been heated up to 65ºC, were it has been found that its deformation at break excesses 600%.[5] In this framework, differential scanning calorimetry (DSC) has been carried out to quantify the bulk crystallinity changes occurring upon drawing. Fig. 1 displays DSC traces of water-quenched PLLA and its stretched counterparts, while Table 1 shows main thermal properties obtained from DSC heating scans. The endothermic overshoot at ~60ºC of specimens is due to physical aging effects during their X-ray study, which was experimentally unavoidable (note that the extent of this endothermic overshoot continuously decreases with stretching ratio because physical aging notably decreases within the crystalline regions).[9] As denoted by the marked heat enthalpy jump, non-stretched polymer shows a glass transition temperature (T_g) at 57.7ºC, followed by an exothermal cold crystallization event cantered at 99.2ºC (T_{cc}) and melting peak located at 175.5ºC (T_m), which agrees well with literature.[5,15,25]
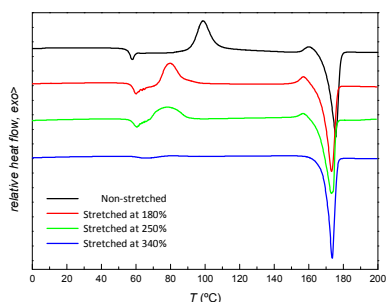
Fig. 1 Heating DSC traces of PLLA stretched for different ratios

Table 1. Thermal properties of stretched. Glass transition temperature (T_g), cold-crystallization enthalpy (ΔH_c), cold-crystallization temperature (T_{cc}), meting temperature (T_m) and crystallinity degree (X_c). N.A.: Not Achieved.

Stretching ratio	T_g (ºC)	ΔH_c (J/g)	T_{cc} (ºC)	T_m (ºC)	X_c (%)	ϕ_c (%)
0 %	57.7	33.3	99.2	175.5	13.2	12.9
180 %	62.3	25.3	79.7	173.1	25.6	25.0
250 %	62.6	8.8	77.1	173.2	43.4	42.4
340 %	64.4	N.A.	N.A.	173.6	56.4	55.5

It is interesting to note that T_g increases by 6.7ºC for stretched specimens, which is associated to a chain confinement behavior induced by the decrease on the amorphous phase as PLLA is further stretched.[5] The confining role of stretch-induced crystallization would successfully delay the fast structural relaxation of polylactides when used at room temperature by reducing chain-conformation changes.[26] A progressive decrease in T_{cc} from 99.2ºC to 77.1ºC as PLLA is further stretched suggests a higher degree of macromolecular orientation which is acting as nuclei to accelerate the cold crystallization process.[27] In a similar way, a less marked cold-crystallization peak is found as polymer is further stretched, which may ascribed to the continuous development of crystalline domains.[5,15] On the contrary, melting temperature of stretched films remains unchanged because crystal size does not change during the stretching.[26] Additionally, the volume crystallinity degree calculated according to Eq. 2 is increased from 12.9% for non-stretched sample to 55.5% for 340% stretched PLLA as a consequence of increased molecular chain alignment induced by drawing.[28]

Conformational analysis by FTIR

Fourier transform infrared spectroscopy (FTIR) has been carried out to provide further insights on the occurring conformational changes upon drawing. Fig. 2a shows normalized (according to carbonyl absorption band located at 1759cm^{-1}) FTIR spectra of non-stretched PLLA and its stretched counterparts (for clarity only most representative spectra are highlighted). The carbonyl (C=O) stretching band is slightly shifted towards higher wavenumbers during the drawing process because the occurring strong dipole–dipole interactions in the densely packed PLLA domains.[4] Moreover, the full width at half maximum (FWHM) of the C=O band decreases from 28.2cm^{-1} for slightly stretched PLLA to 25.4cm^{-1} for 340% stretched PLLA, indicating the formation of new ordered crystalline regions upon drawing.[17] The splitting in the second derivative of the carbonyl stretching band (not shown) highlights a decrease in the amount of amorphous gg conformers (1777 cm^{-1}) together with an increase in the fraction corresponding to gt conformer (1759 cm^{-1}) as a result of the development of crystalline domains as stretching proceeds,[17] which correlates well with obtained DSC results.[29] As shown in Fig. 2b, the band cantered at 922cm^{-1} corresponding to the CH$_3$ rocking mode of PLLA α-form phase (r$_{CH3}$ + v$_{CC}$ mode) notably increases in intensity upon drawing as a expenses of a decrease in the amorphous 955cm^{-1} band (corresponding to CH$_3$ rocking coupled with skeletal C-C stretching in the amorphous phase),[30] denoting a continuous increase on the amount highly-ordered crystalline phases as PLLA is stretched.[4,31] Besides, Fig. 2c shows an increase of the absorption band corresponding to the stretching of C-O-C crystalline group at expenses of the intensity decrease of the amorphous 1265cm^{-1} band further confirms the strain-induced crystallization.[32]

XRD measurements: crystal domain orientation, Pole figures

Wide angle X-ray diffraction experiments were performed to elucidate the occurring structural changes upon stretching. For comparison, cold-crystallizations have been as well carried out to yield the same volume crystalline fraction (DSC traces are shown in Fig. S1) as this heating treatment would produce non-oriented crystalline morphologies.[5,15] As shown in Fig. 3, upon stretching/cold-crystallization noticeable crystal-structure changes take place, which agree with DSC data, where it is shown that PLLA crystallizes upon stretching to yield crystal volume fraction up to
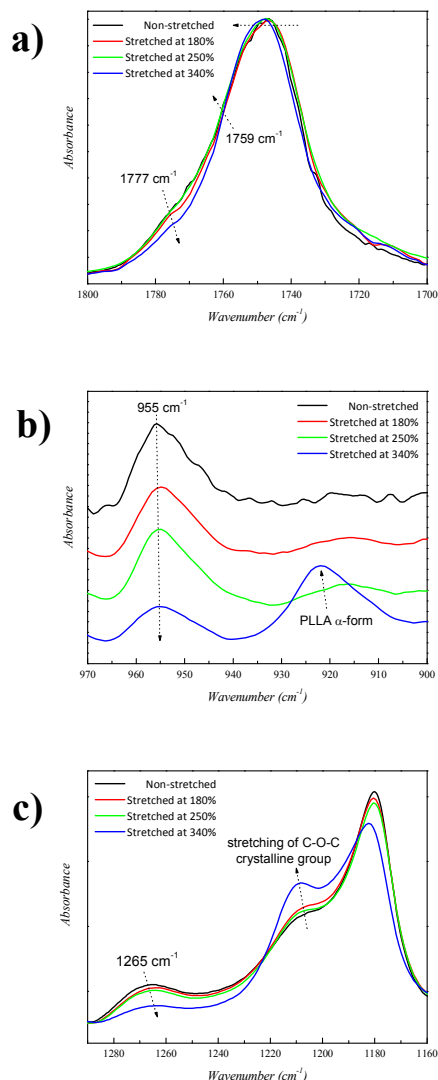
Fig. 2 FTIR spectra for stretched PLLA in the carbonyl (C=O) region (a); crystalline C-O-C group (b) and C-C backbone/CH₃ rocking region (c).

55.5%. Featured reflections of PLLA α´-form corresponding to (110)/(200) and (310)/(200) planes at 2ϑ=16.5º and 28.7º respectively are observed for different stretched sections and for the sample cold-crystallized at 70ºC.[14,33] On the contrary, when PLLA is cold crystallized at temperatures of 100ºC and 110ºC α crystal form is achieved as denoted by the reflections of (010), pointed out that PLLA shows a 10_3 helical conformation when it is crystallized in the α-form,[33] while α´ form could be considered as a *disordered* α-crystal with slightly different lateral packing.[4] In this framework, it is suggested that stretched (and low temperature cold crystallized) PLLA crystallizes into a less-ordered structure because of the rapid crystallization upon drawing imposes external constraints that do not allow the packing of polymeric chains in the more regular 10_3 conformation.[12]
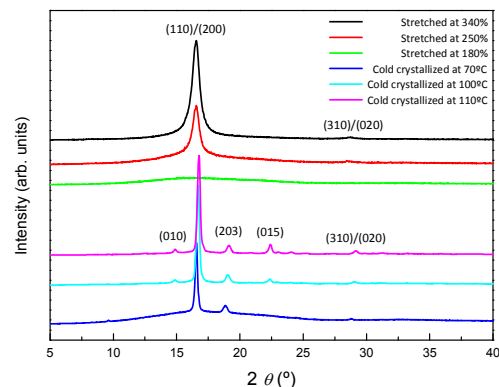
Fig. 3 WAXD patterns for stretched and cold-crystallized PLLA.

The size of crystalline domains could be estimated from the obtained X-ray diffraction patterns the peak width at half height is correlated with the crystal size according to the Scherrer´s equation:[34]

$$\tau = \frac{K \cdot \lambda}{\beta_\tau \cdot \cos\theta} \quad (3)$$

where τ is the average size of crystals, λ is the wavelength of the incident radiation, ϑ is the diffraction angle, K is the Scherrer constant (set at 0.9) and β_τ is the peak width at half height in radians calculated from the main diffraction peak at 2θ~16.8º ($\beta_{Instr.}$ 0.1). Result reveal that the size of developed crystal domains remains unchanged at approximately 10-15Å as stretching proceeds, while crystallite size gradually increases from 61Å to 75Å as cold-crystallization temperature increases from 70ºC to 150ºC, respectively. Those results are in good agreement with DSC data in which it is observed that the melting temperature of PLLA remains unchanged upon stretching, denoting that crystal thickness remains invariable. Obtained crystal-size differences may be explained in terms of molecular mobility differences for PLLA crystallized under uniaxial drawing or by heat treatment. In fact, during the cold crystallization process, polymer chains are reorganized from the mesophase, yielding large crystalline domains because of the increased molecular mobility in comparison with stretch-induced crystallization process, which constraints crystallization process (as discussed above for α and α´ forms). Additionally, macromolecular mobility is larger at 150ºC than at 80ºC, which enables the development of larger crystallites.

It is well known that by drawing a polymer it is possible to obtain a preferential orientation towards the stretching direction of polymeric chains, which in turn would result in outstanding mechanical properties of the resulting material.[35,36] To determine macromolecular orientations texture analysis using XRD has been performed via the Pole figure measurements. Such analysis consists in measuring the intensity of 2 maxima and moving the sample through Psi (tilt) azimuth angle and Phi (spindle) polar rotations via a texture Cradle attachment. The measured intensities are then plotted where the hemisphere-like distribution of scattered intensity is projected (stereographic projection) on a 2D "Pole figure" showing the variation of intensity with the sample

orientation. Measured data were corrected for background scattering and the defocusing of the beam using Multex 3 software.
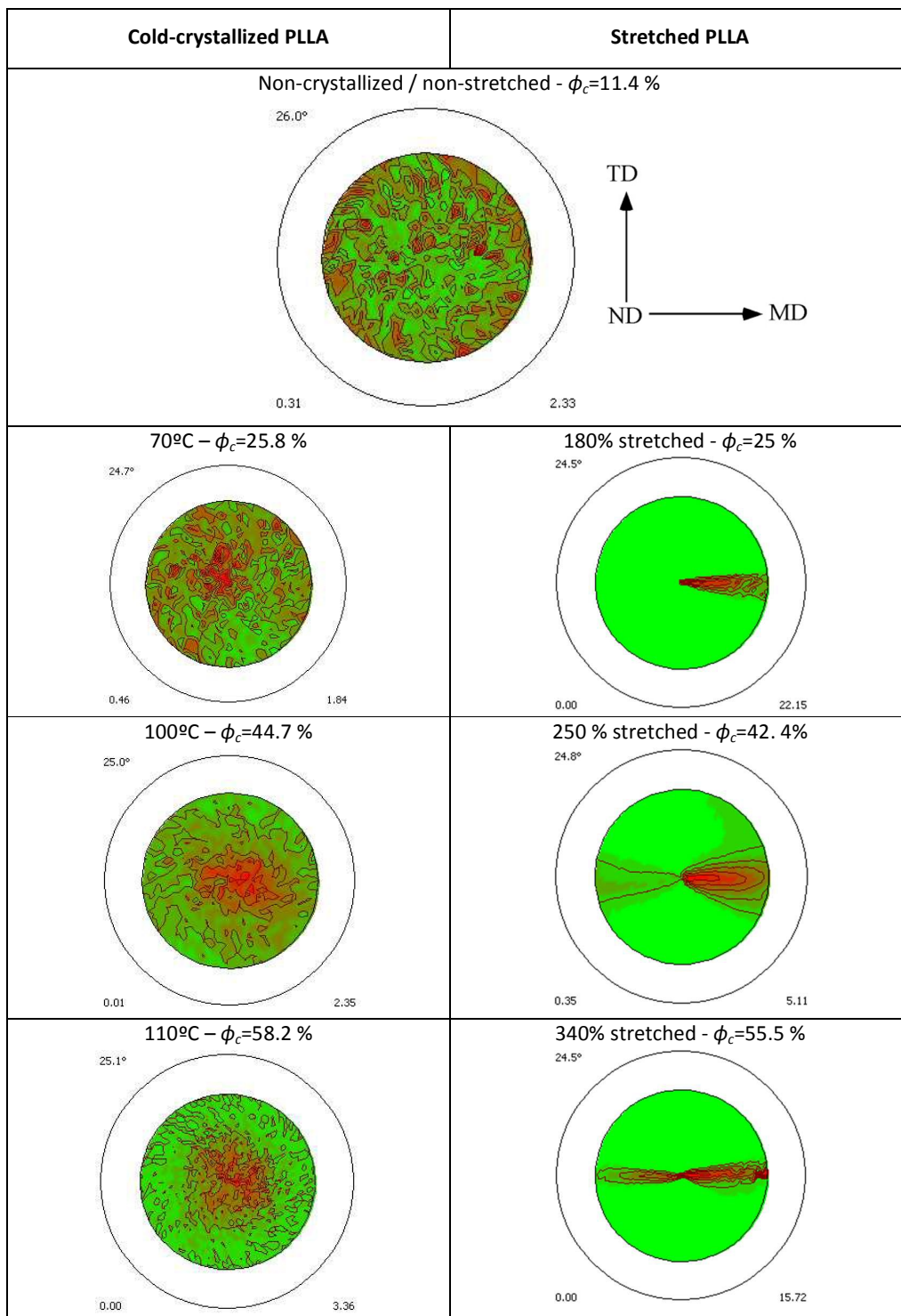
Fig. 4 Obtained pole figures (110)/(200) for different samples with different cold-crystallization temperatures (left column) and stretching ratios (right column). Figures are vertically arranged depending on the achieved crystal volume fractions (φ_c). Note that the relative position (MD/TD) plane of performed pole figures is shown for reference.

Each crystallite in a polycrystalline aggregate has a crystallographic orientation defined in a sample-defined referential. Pole figures are used to describe the variation in the pole density with pole orientation for a selected set of (hkl) crystal planes. A point on the pole figure corresponds to an orientation of the diffraction vector (normal to the diffracting plane) in a coordinate system fixed to the sample. The pole density for a given point is determined by the intensity of X-ray beam diffracted for this orientation. Three orthogonal directions are termed as MD (machine direction) and correlates with stretching direction, TD which represents transversal direction and ND which accounts for the normal direction along the thickness of the sample. In order to fit the obtained Pole figures a model able to simulate the obtained orientations must be created. For these purpose several components, such as fibers (mobiles) and spheres (fixed) have been employed. For the sake of reproducibility, the evaluation of the crystal orientation process was tested by using several samples (see Supporting Information, Fig. S2). Fig. 4 shows the obtained pole figures for stretched and cold-crystallized polymer, giving rise to different crystalline morphologies (crystal volume fractions calculated from the DSC according to Eq. 1 and Eq. 2. are shown above each Pole figure). For comparison very similar bulk volume crystal fractions have been obtained by both crystallization methods. It could be observed that when PLLA is cold-crystallized obtained structure shows a rather isotropic character. On the other hand, the obtained results show that at medium stretching rations PLLA gives crystal volume fractions of about 20-30% (second row) with fibril orientation along the stretching axis (MD axis). Further stretching yield a high amount of well-ordered phases which are oriented not only along the stretching axis but along the MD/ND plane. In fact, it results reasonable to state that upon drawing, crystalline domains are transformed from fibrils in the starting crystallization moments into planar spherulites when the stretching evolves. It is worth to note that depicted Pole figures in the (110)/(200) plane correlate fairly well with the bulk crystal volume

fractions obtained by calorimetry, highlighting the high reproducibility of achieved results.

To shed more light on the occurring strain-induced three-dimensional crystal orientation, it results essential to understand how are correlated the three-dimensional stress/strain in isotropic materials. In this framework, according to the Hooke´s Law,[37] which is applied to isotropic materials, the strain in the *x*, *y* and *z* directions (ε_{xx}, ε_{yy} and ε_{zz} respectively) is defined in terms of Young´s modulus and Poisson´s ratio as:

$$\varepsilon_{xx} = \frac{1}{E}\left[\sigma_{xx} - \upsilon(\sigma_{yy} + \sigma_{zz})\right] \tag{4}$$

$$\varepsilon_{yy} = \frac{1}{E}\left[\sigma_{yy} - \upsilon(\sigma_{xx} + \sigma_{zz})\right] \tag{5}$$

$$\varepsilon_{zz} = \frac{1}{E}\left[\sigma_{zz} - \upsilon(\sigma_{xx} + \sigma_{zz})\right] \tag{6}$$

where *E* is the Young´s modulus and σ_{xx}, σ_{yy} and σ_{zz} are the applied stresses in *x*, *y* and *z* directions. υ is the Poisson´s ratio, that for a commercial PLLA has been found to be 0.36,[38] which falls in the typical range of isotropic engineering materials (Poisson's ratio between 0.2 and 0.5).[39] Poisson´s ratio represents the negative relationship of transverse to axial strain, indicating the extent of lateral compression when PLLA is stretched. In other words, at the same time that the polymer is stretched along its longitudinal direction, it is continuously being compressed along its transversal direction.

Additionally, taking in to account the PLLA α-form crystal lattice constants (orthorhombic unit cell with 10.70 Å, 6.20 Å, 28.86Å, 90.0°, 90.0°, 90.0°),[4,33] the sample symmetry (Schoenfliess notation D2) and the used Bragg Reflection (200), the most stretched section can be simulate by using a fiber component (h=(90.0°, 90.0°) f=(90.3°, 91.4°)) that gives rise to planar spherulitic morphology (MD/ND) perpendicular to the shortening axis (TD). As illustrated in Fig. 5, this behavior is in good agreement with the assumption that the extensional flow could be more effective in aligning the polymer chains. Less stretched samples presents a limited disc sections of the planar spherulitic morphology orientations that can be simulated using different number of Sphere type components, g=(90.0°,94.0-160°,90.0°).
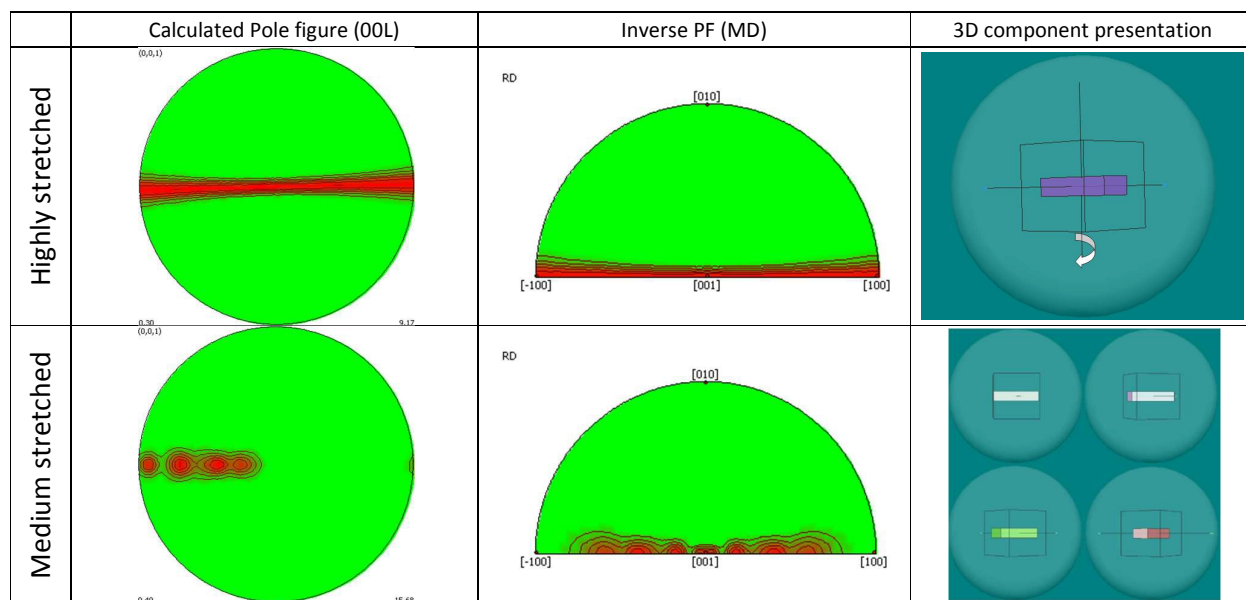
Fig. 5 Pole figure calculations using fiber and sphere components, for highly and medium stretched section, respectively.

Morphological observations of crystallized samples

FE-SEM studies were performed to obtain morphological evidences for the suggested crystal transformations. For clarity, a model depicting the relative position of analyzed sections is shown in Supporting Information (Fig. S3). Remarkable morphological differences are achieved between non cold-crystallized/stretched, cold-crystallized and stretched PLLA. As shown in Fig. 6a, non cold-crystallized/non-stretched polymer shows smooth surface because of the characteristic brittle nature of PLLA.[5,40] It could be observed that PLLA develops rougher structures upon increasing cold-crystallization temperature. Moreover, cold-crystallization process yields randomly distributed crystallites as observed in Fig. 6b-c, which agrees well with pole figures depicted in Fig. 4, where it is demonstrated that after cold-crystallization of PLLA an isotropic crystalline structure is developed. On the contrary, as highlighted in Fig. 6d-e, as stretching proceeds the initially amorphous material continuously evolves towards anisotropically arranged crystalline domains, increasing the amount of crystals for higher stretching ratios according to obtained DSC and WAXD data. Furthermore, observed domains in Fig. 6d and Fig. 6e could be identified as the projection of planar spherulites onto a ND/TD plane, which is consistent with measured pole figures (see Fig. 4).

To obtain further evidences on the morphology of formed crystals during PLLA stretching, further FE-SEM analysis were carried out in the stretching plane (perpendicular to images showed in Fig. 6; see Fig. S4). Acquired images clearly demonstrate that upon stretching crystalline domains are transformed from fibrils in
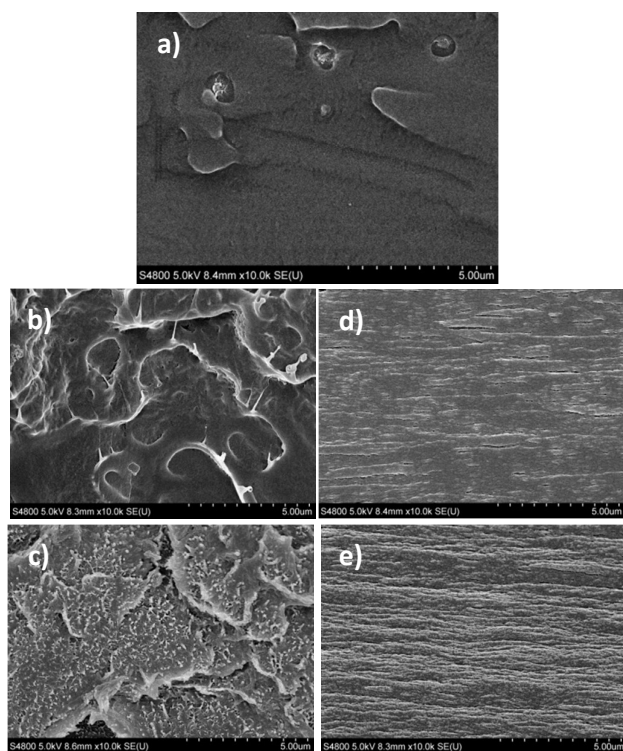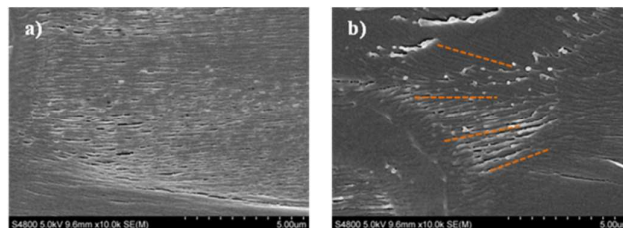
Fig. 7 FE-SEM micrographs of cryogenically fractured PLLA showing fibril morphology (a) and planar spherulites (b) upon stretching.

the starting crystallization moments (Fig. 7a) into planar spherulitic morphology (Fig. 7b), where the radial growth direction is highlighted with orange dotted lines.

Strain-induced crystallization mechanism

Taking into account obtained experimental findings, the occurring three-dimensional stress/strain relationships in isotropic materials (Hooke´s Law) and the 2D Pole figure calculation shown in Fig. 5, a schematical representation concerning the strain-induced crystallization mechanism upon stretching is proposed in Fig. 8. For that, it should be taken into account that when polymers are crystallized from the melt the macromolecular chains have enough mobility to form well-ordered regions called spherulites, which are three-dimensional supramolecular structures with usual diameters of 5-40μm for PLLA.[5] On the contrary, in this work and according to Hooke´s Law, the externally imposed constrains upon stretching in ND (slight compressive), TD (intense compressive) and MD (intense tensile) directions decrease the number of degrees of freedom for crystallization process, avoiding the crystallization of three-dimensional polylactide crystals (in accordance with WAXD data, which reveals that stretching produces small crystallites of about 10-15nm with α´ packing mode). Thus, at low stretching ratios (crystal volume fractions of 20-30%) only few crystalline regions are oriented along the MD axis, which represents the stretching direction, which are surrounded by extensive amorphous regions as depicted by pink lines. Increasing applied stress yields further crystalline domains (crystal volume of ~55%) that are oriented not only along the MD axis but in the MD/ND plane (planar spherulites), as schematically presented in the Fig. 8.

Fig. 6 FE-SEM micrographs of cryogenically fractured PLLA surfaces obtained at a magnification of 10.000X: a) non cold-crystallized/stretched PLLA; b) cold crystallized at 70ºC; c) cold crystallized at 150ºC; d) stretched for 180% and e) stretched for 340%.
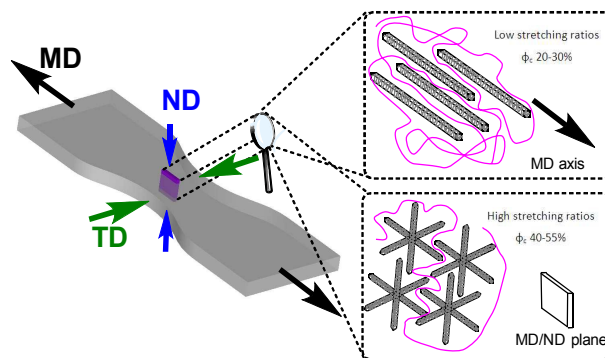
Fig. 8 Schematic representation showing the applied strain along three directions (MD, ND and TD corresponding to ε_{xx}, ε_{yy} and ε_{zz} respectively) and the corresponding 3D-crystal formation for low and highly stretched PLLA.

Conclusions

Up to date, the determination of crystallographic orientations by pole figures has been mainly limited to inorganic materials. Thorough this work we have found interesting results towards the understanding of the occurring chain orientation effects during PLLA stretching, for which very scarce studies could be found in polymer science. Poly (L-lactide) has been submitted to different stretching ratios at 65ºC to ensure an elastomeric behavior while avoiding temperature-induced crystallization, obtaining bulk crystal volume fractions up to 55.5%.

DSC results show a T_g increase of 6.7ºC for stretched specimens associated to a chain confinement induced by the presence of evolving ordered domains. FTIR results reveal increased dipole–dipole interactions with stretching as a result of highly-ordered crystalline phases as polymer is stretched. Structural changes upon stretching have been confirmed by wide angle X-ray diffraction analysis. Additionally, to determine macromolecular orientations texture analysis has been performed via the pole figure measurements in the (110)/(200) plane. Results suggest that upon stretching crystalline domains are transformed from fibrils in the starting crystallization moments into planar spherulitic morphology perpendicular to the shortening biggest axis. Experimentally obtained 2D Pole figures correlate fairly well with the bulk crystal volume fractions obtained by calorimetry, highlighting the high reproducibility of the achieved results. Obtained morphological evidences for the suggested crystal transformations further confirm our hypothesis.

A model depicting the strain-induced three-dimensional crystal orientation is developed on the basis of the obtained Pole figures. According to it, the externally imposed constrains upon stretching in both longitudinal and transversal directions decrease the number of degrees of freedom for crystallization process, avoiding the crystallization of three-dimensional polylactide crystals. Thus, while low stretching ratios result in few crystalline regions oriented along the MD axis, an increase in the applied stress yields further crystalline domains that are oriented not along the MD axis but in the MD/ND plane.

In overall, obtained experimental results together with the proposed model for strain-induced three-dimensional crystalline development are expected to provide a deeper comprehension on how conventional thermoplastic processing techniques induce microstructural changes in semicrystalline polymers.

Acknowledgements

Notes and references

1   R. Auras, B. Harte and S. Selke, *Macromol. Biosci.* 2004, **4**, 835-864.
2   D. J. Garlotta, *J. Polym. Environ.* 2001, **9**, 63-84.
3   I. Diddens, B. Murphy, M. Krisch and M. Muller, *Macromolecules* 2008, **41**, 9755-9759.
4   E. Meaurio, I. Martinez de Arenaza, E. Lizundia and J. R. Sarasua, *Macromolecules* 2009, **42**, 5717–5727.
5   E. Lizundia, S. Petisco and J. R. Sarasua, *J. Mech. Behav. Biomed. Mater.* 2013, **17**, 242-251.
6   C. Chaiwong, P. Rachtanaprun, P. Wongchaiya, R. Auras and D. Boonyawan, *Surf. Coat. Tech.* 2010, **240**, 2933-2939.
7   J. W. Rhim, S. I. Hong and C. S. Ha, *Food Sci. Technol.* 2009, **42**, 612-617.
8   X. Hu, H. Xu and Z. Li, *Macromol. Mater. Eng.* 2007, **292**, 646-654.
9   E. Lizundia and J. R. Sarasua, *Macromol. Symp.* 2012, **321-322**, 118–123.
10 A. P. Gupta and V. Kumar, *Eur. Polym. J.* 2007, **43**, 4053-4074.
11 T. Miyata and T. Masuko, *Polymer* 1998, **39**, 5515–5521.
12 L. Cartier, T. Okihara, Y. Ikada, H. Tsuji, J. Puiggali and B. Lotz, *Polymer* 2000, **41**, 8909–8919.
13 M. O. Oh and S. H. Kim, *Polym. Int.* 2014, **63**, 1247-1253.
14 G. Liu, X. Zhang and D. Wang, *Adv. Mater.* 2014, **26**, 6905–6911.
15 J. del Rio, A. Etxeberria, N. Lopez-Rodriguez, E. Lizundia and J. R. Sarasua, *Macromolecules* 2010, **43**, 4698-4707.
16 T. D. Fornes and D. R. Paul, *Polymer* 2003, **44**, 3945-3961.
17 E. Meaurio, E. Zuza, N. Lopez-Rodriguez and J. R. Sarasua, *J. Phys Chem. B* 2006, **110**, 5790-5800.
18 E. W. Bohannan, H. M. Kothari, I. M. Nicic and J. A. Switzer, *J. Am. Chem. Soc.* 2004, **126**, 488–489.
19 H. Itahara, W. S. Seo, S. Lee, H. Nozaki, T. Tani and K. Koumoto, *J. Am. Chem. Soc.* 2005, **127**, 6367–6373.
20 O. Lyandres, D. Finkelstein-Shapiro, P. Chakthranont, M. Graham and K. A. Gray, *Chem. Mater.* 2012, **24**, 3355–3362.
21 S. Boonsalee, R. V. Gudavarthy, E. W. Bohannan and J. A. Switzer, *Chem. Mater.* 2008, **20**, 5737–5742.
22 P. T. Anastas and J. C. Warner, Green Chemistry: Theory and Practice; Oxford University Press. New York 1998, 148.
23 E. W. Fischer, H. J. Sterzel and G. Wegner, *Kolloid-Zu Z-Polymer* 1973, **251**, 980–990.
24 D. Sawai, Y. Tsugane, M. Tamada, T. Kanamoto, M. Sungil and S. Hyon, *J. Polym. Sci. Part B: Polym. Phys.* 2007, **45**, 2632-2639.
25 E. Lizundia, A. Oleaga, A. Salazar and J. R. Sarasua, *Polymer* 2012, **53**, 2412-2421.
26 E. Lizundia, J. L. Vilas and L. M. León, *Carbohydr. Polym.* 2015, **123C**, 256-265.
27 B. Na, J. Zhu, R. Lv, P. Zhang and Q. Liu, *J. Appl. Polym. Sci.* 2014, **131**, 39993.
28 R. Hiss, S. Hobeika, C. Lynn and G. Strobl, *Macromolecules* 1999, **32**, 4390–4403.
29 J. Zhang, Y. Duan, H. Sato, H. Tsuji, I. Noda, S. Yan and Y. Ozaki, *Macromolecules* 2005, **38**, 8012-8021.
30 M. Jamshidian, E. A. Tehrany, M. Imran, M. Jacquot and D. Desobry, *Compr. Rev. Food Sc. F.* 2010, **9**, 552-571.
31 J. M. Zhang, H. Tsuji, I. Noda and Y. Ozaki, *Macromolecules* 2004, **37**, 6433–6439.
32 T. Furukawa, H. Sato, R. Murakami, J. Zhang, Y. Duan, I. Noda, S. Ochiai and Y. Ozaki, *Macromolecules* 2005, **38**, 6445-6454.
33 K. Wasanasuk, K. Tashiro, M. Hanesaka, T. Ohhara, K. Kurihara, R. Kuroki, T. Tamada, T. Ozeki and T. Kanamoto, *Macromolecules* 2011, **44**, 6441–6452.
34 D. Brizzolara, H. J. Cantow, K. Diederichs, E. Keller and A. J. Domb, *Macromolecules* 1996, **29**, 191-197.
35 G. Stoclet, R. Seguela, C. Vanmansart, C. Rochas and J. M. Lefebvre, *Polymer* 2012, **53**, 519-528.

Please **RSC Advances** argins

36 H. Tsuji, *Macromol. Biosci*. 2005, **5**, 569–597.

37 A. C. Ugural and S. K. Fenster, Advanced Mechanics of Materials and Applied Elasticity (4th Edition). Prentice Hall, Englewood Cliffs, N.J., 2003.

38 M. Jamshidian, E. A. Tehrany, M. Imran, M. Jacquot and D. Desobry, *Compr. Rev. Food Sc. F.* 2010, **9**, 552-571.

39 P. H. Mott and C. M. Roland, *Phys. Rev. B.* 2009, **80**, 132104.

40 E. Lizundia, E. Meaurio, J. M. Laza, J. L. Vilas and L. M. León, *Mater. Sci. Eng., C* 2015, **50**, 97-106.

Graphical Abstract

Three-dimensional orientation of Poly(L-lactide) crystals under uniaxial drawing

Erlantz Lizundia, Aitor Larrañaga, José L. Vilas, Luis M. León

Slightly stretched   Highly stretched

Fibrils alond MD axis

Planar spherulites
along MD/ND plane